

## Origin of the insulating state in honeycomb iridates and rhodates

I. I. Mazin,<sup>1</sup> S. Manni,<sup>2</sup> K. Foyevtsova,<sup>3,\*</sup> Harald O. Jeschke,<sup>3</sup> P. Gegenwart,<sup>2</sup> and Roser Valentí<sup>3</sup>

<sup>1</sup>Code 6393, Naval Research Laboratory, Washington, D.C. 20375, USA

<sup>2</sup>I. Physikalisches Institut, Georg-August-Universität Göttingen, 37077 Göttingen, Germany

<sup>3</sup>Institut für Theoretische Physik, Goethe-Universität Frankfurt, 60438 Frankfurt am Main, Germany

(Received 8 April 2013; revised manuscript received 10 June 2013; published 12 July 2013)

A burning question in the emerging field of spin-orbit driven insulating iridates, such as  $\text{Na}_2\text{IrO}_3$  and  $\text{Li}_2\text{IrO}_3$ , is whether the observed insulating state should be classified as a Mott-Hubbard insulator derived from a half-filled relativistic  $j_{\text{eff}} = 1/2$  band or as a band insulator where the gap is assisted by spin-orbit interaction or Coulomb correlations or both. The difference between these two interpretations is that only for the former strong spin-orbit coupling ( $\lambda \gtrsim W$ , where  $W$  is the bandwidth) is essential. We have synthesized the isostructural and isoelectronic  $\text{Li}_2\text{RhO}_3$  and report its electrical resistivity and magnetic susceptibility. Remarkably, it shows insulating behavior together with fluctuating effective  $S = 1/2$  moments, similar to  $\text{Na}_2\text{IrO}_3$  and  $\text{Li}_2\text{IrO}_3$ , although in  $\text{Rh}^{4+}$  ( $4d^5$ ) the spin-orbit coupling is greatly reduced. We show that this behavior has a nonrelativistic one-electron origin (although Coulomb correlations assist in opening the gap) and can be traced to the formation of quasimolecular orbitals, similar to those in  $\text{Na}_2\text{IrO}_3$ .

DOI: [10.1103/PhysRevB.88.035115](https://doi.org/10.1103/PhysRevB.88.035115)

PACS number(s): 75.10.Jm, 71.70.Ej, 71.15.Mb

In recent years, complex iridium oxides have caused extraordinary interest<sup>1–4</sup> since the physics there is governed by a unique combination of several comparable scales: one-electron hopping  $t$ , spin-orbit coupling (SOC)  $\lambda$ , and the Hubbard repulsion  $U$ . The honeycomb layered compound  $\text{Na}_2\text{IrO}_3$ , a small-gap antiferromagnetic (AFM) insulator,<sup>5,6</sup> has received particular attention. It was suggested that the adequate description of the electronic behavior of this system is in terms of a half-filled relativistic  $j_{\text{eff}} = 1/2$  band, which becomes a Mott-Hubbard insulator.<sup>7</sup> However,  $U$  in iridates is rather small (1.5–2 eV), and therefore the corresponding band must be rather narrow for the system to become insulating. In this scenario, the SOC is the leading interaction in these systems, so that the  $t_{2g}$  bands split into a narrow doublet with the effective angular momentum  $j_{\text{eff}} = 1/2$  and a quartet with  $j_{\text{eff}} = 3/2$ . In the idealized crystal structure, the one-electron hopping between the doublet states is fully suppressed, and the effect of one-electron hopping is reduced, by perturbation theory, to the second order in  $t$ , that is, to  $t^2/1.5\lambda \sim t/3$ , where  $1.5\lambda$  is the energy separation between the doublet and the quartet.

Recently, Mazin *et al.*<sup>8</sup> proposed an alternative description and argued that the one-electron nonrelativistic band structure might be a better starting point for the description of the electronic behavior of honeycomb iridates than the limit  $\lambda \gg W$  (bandwidth). In this case the band structure is dominated by the formation of so-called quasimolecular orbitals (QMOs) and consists of four narrow bands (the width being defined by second-neighbor hoppings and other secondary one-electron parameters), spread over a width of  $\sim 4t$ , where  $t \sim 0.3$  eV is the leading one-electron hopping. The highest and the lowest bands are singlets, having one state per two Ir (i.e., one state per spin per unit cell of two formula units), and the two middle bands are doublets. In the  $\lambda = 0$  limit the upper singlet and doublet bands nearly merge, forming a triplet manifold, while turning on SOC further splits those bands into three singlets. The upper two bands barely overlap, forming an incipient (SOC assisted) band insulator, and even

a very small  $U$  of a few tenths of an eV is sufficient to open a gap. In this picture, the material is characterized as a spin-orbit assisted insulator with the gap enhanced by Hubbard correlation.

In view of the two alternative, and partly opposite, descriptions of the insulating state in these systems, we present here a comparative analysis between the electronic behavior of hexagonal iridates and rhodates. Specifically, we have synthesized and investigated  $\text{Li}_2\text{RhO}_3$ , which shows insulating behavior at low temperatures, similar to  $\text{Na}_2\text{IrO}_3$  and  $\text{Li}_2\text{IrO}_3$ , even though in  $\text{Rh}^{4+}$  ( $4d^5$ ) the SOC is substantially reduced. The comparison sheds light onto the nature of the insulating state in these systems.

The paper is organized as follows. We first settle the terminology between the various definitions of insulators. We then proceed with electrical resistivity and magnetic susceptibility data of  $\text{Li}_2\text{RhO}_3$  and the description of its electronic and magnetic properties by means of density-functional theory (DFT) calculations with and without inclusion of spin-orbit coupling and discuss the similarities and differences of this rhodate system compared to the hexagonal iridates. As an outlook, we provide some predictions for the magnetism in the hexagonal rhodates.

The question of whether a particular phase is characterized as a Mott-Hubbard insulator or a band insulator is largely terminological, as no strict definition or criterion exists to rigorously separate these notions. Some authors<sup>9</sup> further subdivide the classification of insulators into Peierls, Wilson, Slater, or Hund insulators, to mention a few. We feel that this fine tuning is not helpful here, and we will concentrate on the difference between Mott and band insulators, which is fundamental in the sense that one cannot go from the former to the latter continuously. Note that this division does not have a one-to-one correspondence with the strongly-correlated–weakly-correlated dichotomy; a band insulator, in our terminology, may have a gap strongly enhanced by correlations but is still “topologically connected” with an uncorrelated insulator.

We can illustrate this with a simple example: imagine a crystal of atoms with one half-occupied orbital. If the crystal has one atom per unit cell, then on the one-electron level this material can never be insulating. Upon including an onsite Hubbard  $U$ , thereby penalizing double occupation and hindering itinerancy, it becomes a *Mott insulator*,<sup>10,11</sup> with no coherent quasiparticles. This happens roughly when  $U$  becomes larger than the total bandwidth  $W$ . Now, suppose the same atoms are bound in dimers forming a molecular crystal. Each dimer develops a bonding and an antibonding state split by some energy  $\Delta$ . We now allow interdimer hopping. The levels will broaden into bonding and antibonding bands of the width  $W$ . As long as  $W < \Delta$ , the material is a *band insulator*. If  $\Delta \sim W$ , the gap is very small, and the indirect gap may even become negative. If we add a Hubbard  $U$  to this system (not necessarily larger than  $W$ ) the gap will get larger by some fraction of  $U$  (depending on the degree of itinerancy), and this may be a substantial enhancement. We call this a *correlation-enhanced band insulator*. For instance, solid Ne is a band insulator, even though in local-density approximation (LDA) calculations its gap is severely underestimated (12.7 vs 21.4 eV).<sup>12</sup> This discrepancy is related to another problem in the density-functional theory (DFT), the so-called density derivative discontinuity, and not to Hubbard correlations. To first approximation, this discrepancy is inversely proportional to the static dielectric function.<sup>13</sup>

An example of a Mott insulator is FeO. It has one electron in the spin-minority  $t_{2g}$  band and is a metal in DFT. Coulomb correlations have to destroy entirely the coherent DFT metallic band crossing the Fermi level, and the excitation gap appears between the incoherent lower and upper Hubbard band.<sup>14</sup> Note that despite FeO being a Mott insulator even in the paramagnetic phase the simplistic treatment of LDA +  $U$ ,<sup>15</sup> as opposed to more sophisticated dynamical mean-field theory (DMFT),<sup>14</sup> cannot reproduce insulating behavior by symmetry; the cubic symmetry needs to be broken, for instance, by assuming antiferromagnetic ordering, after which a gap opens at sufficiently large values of  $U$ . Similarly, in parent compounds of the superconducting cuprates there exists one hole in the  $e_g$  band, and symmetry does not allow one to open a gap in DFT. These systems are “true” Mott-Hubbard insulators.

Finally, MnO is an example of a (strongly) correlation-enhanced band insulator. It has a gap between  $3d$  majority and minority bands. In DFT, this gap is driven by Hund’s rule and is  $\sim 5I - W$ , where the Stoner factor  $I$  is  $\sim 1$  eV. The calculated value is 1.4 eV as compared to 4.5 eV in the experiment.<sup>16</sup> This material is strongly affected by Mott physics and routinely called a Mott insulator, yet one can make a gedanken experiment and gradually reduce the Hubbard correlations to zero, whereupon the gap will drop to its DFT value, without losing the insulating character. Note also that a Mott-Hubbard insulator, in our nomenclature, does not necessarily imply a strong Hubbard repulsion  $U \gg t$ , where  $t$  is a typical intersite hopping. For instance, TaS<sub>2</sub> by no means can be expected to be a strongly correlated material, and  $U$  cannot be more than a fraction of an eV, and, indeed, at high temperatures it is a metal. Yet at low temperature it experiences a charge-density wave transition typical for this structure, which, combined with the spin-orbit interaction on

Ta, splits off, essentially accidentally, an ultranarrow band ( $W \sim 0.1$  eV), and even a minuscule  $U$  suffices to split it into two Hubbard bands.

In Na<sub>2</sub>IrO<sub>3</sub>,  $U$  is relatively small and the material cannot be strongly correlated. Moreover, correlations are suppressed in LDA +  $U$  calculations because of substantial delocalization of electrons over Ir<sub>6</sub> hexagons, so that in order to increase the calculated gap from  $\sim 0$  to  $\sim 0.3$  eV one has to add  $U \sim 4$  eV. Furthermore, there is indirect evidence of itinerancy in the experiment: the ordered magnetic moment even at the lowest temperature is less than  $0.3\mu_B$ ,<sup>17</sup> in reasonable agreement with the band-structure calculations ( $\approx 0.5\mu_B$ , equally distributed between spin and orbital moments), while the fully localized  $j_{\text{eff}}$  model ( $1\mu_B$ , split 2:1 between spin and orbital moments) requires strong fluctuations to suppress the ordered moment.<sup>18</sup>

It is often argued that the experimentally measured<sup>19</sup> spin-orbit correlation factor,  $\langle \mathbf{L} \cdot \mathbf{S} \rangle$ , is consistent with one hole in the  $j_{\text{eff}} = 1/2$  state and thus proves its existence. However, this factor is mostly collected from the  $e_g$  holes<sup>20,21</sup> and is well described by band-structure calculations.

A comparison of honeycomb iridates with the isostructural and isoelectronic Li<sub>2</sub>RhO<sub>3</sub> should be very instructive, because if the former are SOC Mott insulators like Sr<sub>2</sub>IrO<sub>4</sub>,<sup>3,22</sup> then a Rh analog (with much weaker SOC) should be metallic, just as Sr<sub>2</sub>RhO<sub>4</sub>.<sup>23</sup> If, on the other hand, the formation of quasimolecular orbitals triggers the insulating behavior, then a larger  $U$  in Li<sub>2</sub>RhO<sub>3</sub> will likely recreate the same physics as for Na<sub>2</sub>IrO<sub>3</sub>, i.e., a correlation-enhanced band insulator.

We have synthesized Li<sub>2</sub>RhO<sub>3</sub> polycrystals by the solid-state reaction method from stoichiometric amounts of Li<sub>2</sub>CO<sub>3</sub> and Rh powder. The mixture has several times been pelletized and reacted in O<sub>2</sub> flow at temperatures up to 850 °C. Powder x-ray-diffraction (XRD) scans do not reveal any evidence for secondary phases and are similar to those reported in Ref. 24 (cf. Fig. 3). Magnetic susceptibility and (four-probe) electrical resistivity have been determined utilizing commercial (Quantum Design) instruments.

As presented in Fig. 1(a), Li<sub>2</sub>RhO<sub>3</sub> shows clear insulating resistivity behavior, which follows the same variable-range hopping dependence as found in Na<sub>2</sub>IrO<sub>3</sub> or Li<sub>2</sub>IrO<sub>3</sub>.<sup>5,25</sup> Previous resistivity measurements at higher temperatures found an activation gap of  $\sim 80$  meV.<sup>24</sup> The magnetic susceptibility [Fig. 1(b)] is Curie-Weiss (CW) like, with a small kink at 6 K, likely due to some spin-glass freezing, which needs to be investigated in future measurements. The CW fit between 100 and 300 K corresponds to  $\mu_{\text{eff}} = 2.2\mu_B$ . Similar results have been recently reported by Luo *et al.*<sup>26</sup>

Now, we need to establish the crystal structure. Lab powder XRD is not very sensitive to the O positions, which hinders structural determination. For instance, initial powder XRD refinement for Na<sub>2</sub>IrO<sub>3</sub><sup>5</sup> was unable to distinguish between  $C2/c$  and  $C2/m$  structure, but later measurements on a single crystal showed that  $C2/m$  is the most stable crystal structure with well-ordered regular honeycomb planes.<sup>17</sup> Also, for Li<sub>2</sub>RhO<sub>3</sub> there has been discussion about Li-Rh site exchange.<sup>24</sup> However, we have found that site exchange and stacking faults have similar effects on powder XRD Rietveld refinement. Thus, from the present data it is very hard to distinguish between them. On the other hand,

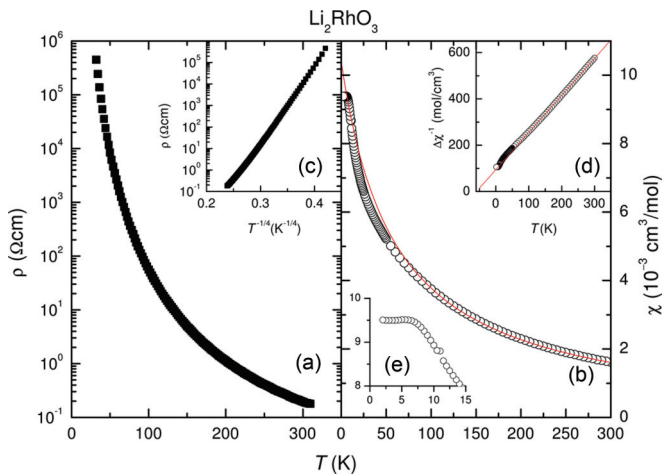


FIG. 1. (Color online) Temperature dependence of the electrical resistivity (a) and magnetic susceptibility (b) of polycrystalline  $\text{Li}_2\text{RhO}_3$ . Inset (c) displays the resistivity data (on log scale) vs  $T^{-1/4}$ . The line in (b) is a Curie-Weiss (CW) fit  $\chi(T) = \chi_0 + C/(T - \Theta_W)$  with  $\chi_0 = -1.235 \times 10^{-4} \text{ cm}^3/\text{mol}$  and  $\Theta_W = -59 \text{ K}$ . Inset (d) shows  $\Delta\chi^{-1}$  vs  $T$  with  $\Delta\chi = \chi(T) - \chi_0$  and the CW fit. Inset (e) displays the same data as in (b) for the low-temperature regime.

single-crystal XRD on  $\text{Na}_2\text{IrO}_3$  by Choi *et al.* found evidence that stacking faults are the leading defects rather than Na-Ir site exchange.<sup>17</sup>

For that reason, we have used (well-determined) unit-cell parameters for  $\text{Li}_2\text{RhO}_3$  and performed first-principles optimization of the internal parameters.<sup>27</sup> We note that the same procedure yielded excellent agreement with the refined crystal structure of  $\text{Na}_2\text{IrO}_3$ .<sup>17</sup> The final structure is presented in Table I and shown in Fig. 2. This refined structure is consistent with the laboratory powder XRD data (Fig. 3).

Despite the overall low crystal symmetry, the local symmetry of the  $\text{Rh}_2\text{Li}$  planes is rather high: the hexagons are nearly ideal and the Rh-O-Rh angles are nearly the same and relatively close to  $90^\circ$ . This makes it a showcase for the quasimolecular orbital concept.<sup>8</sup> To this end, we

TABLE I. Optimized crystal structure of  $\text{Li}_2\text{RhO}_3$ , using experimental lattice parameters ( $a = 5.123 \text{ \AA}$ ,  $b = 8.836 \text{ \AA}$ ,  $c = 5.885 \text{ \AA}$ ,  $\beta = 125.374^\circ$ ) and space group  $C2/m$ . The nearest neighbor Rh-Rh and Rh-O distances as well as Rh-O-Rh angles are given. Note that the hexagon structure is not perfect and there are two Rh-Rh and three Rh-O nearest neighbours.

Atom	Position	$x$	$y$	$z$
Rh	$4h$	0	0.333	1/2
Li	$2a$	0	0	0
Li	$4g$	0	0.660	0
Li	$2c$	0	0	1/2
O	$8j$	0.516	0.327	0.263
O	$4i$	0.002	1/2	0.7380
		dist./angle 1	dist./angle 2	dist. 3
Rh-Rh		2.951 $\text{\AA}$	2.952 $\text{\AA}$	
Rh-O		2.023 $\text{\AA}$	2.030 $\text{\AA}$	2.021 $\text{\AA}$
Rh-O-Rh		93.2 $^\circ$	93.8 $^\circ$	

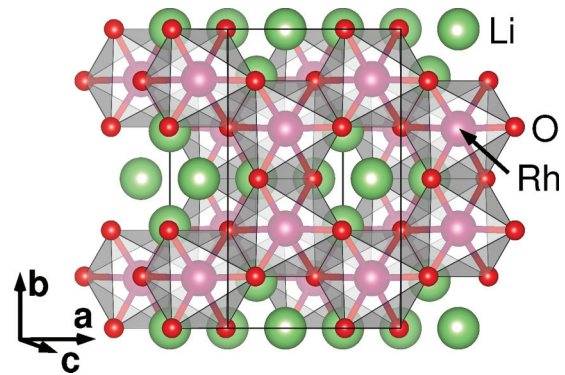


FIG. 2. (Color online) Structure of  $\text{Li}_2\text{RhO}_3$ , viewed along the  $c$  direction.

have performed first-principles calculations using the WIEN2K code<sup>28</sup> and projected the results using a standard Wannier function projection technique as proposed by Aichhorn *et al.*<sup>29</sup> and further developed in Ref. 30. The resulting tight-binding parameters are shown in Table II.

As we see, the main condition for the QMO picture (dominance of the O-assisted nearest-neighbor hoppings) is fulfilled. Projecting the density of states (DOS) onto individual QMOs we see that, although it does not separate into isolated manifolds as in  $\text{Na}_2\text{IrO}_3$ , it is composed of overlapping QMOs as shown in Fig. 4.

We have also performed spin-polarized calculations with various spin configurations<sup>31</sup> [Fig. 5(a)]. We were not able to stabilize a Néel order (magnetic moments collapse), but the ferromagnetic (FM) and two antiferromagnetic phases, the “stripy” and the “zigzag” phases, are all stable, with the ground state practically degenerate between the two AFM states. The FM state has a small advantage in the calculations, which is lost upon application of  $U$  (see below). The calculated FM state, just as in  $\text{Na}_2\text{IrO}_3$ , is a half metal with  $M = 1\mu_B/\text{Rh}$ . One has to keep in mind that at small  $U$  the material is metallic, which promotes ferromagnetism, and that LDA and generalized gradient approximation (GGA) include

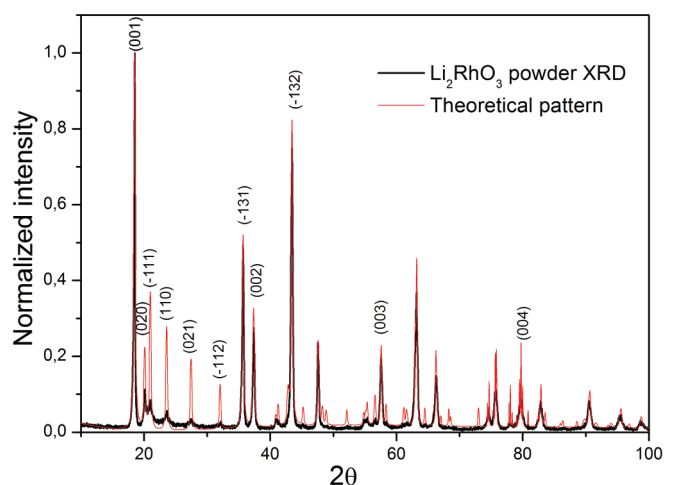


FIG. 3. (Color online) Comparison of observed (black) and calculated (red) powder XRD spectra for  $\text{Li}_2\text{RhO}_3$  (see text).

TABLE II. Comparison of the first-principles hopping amplitudes in  $\text{Li}_2\text{RhO}_3$  and  $\text{Na}_2\text{IrO}_3$ . The notations are explained in detail in Ref. 21. All hoppings  $t$  and onsite energies  $\mu$  are given in meV.

	$\text{Na}_2\text{IrO}_3$		$\text{Li}_2\text{RhO}_3$	
$\mu^{xy}$	-448.8		-385.8	
$\mu^{xz,yz}$	-421.5		-385.7	
$t_0^{xy \rightarrow xz,yz}$	-27.8		-18.8	
$t_0^{xz \rightarrow yz}$	-23.1		-15.5	
Distance	3.130 Å	3.138 Å	2.951 Å	2.952 Å
$t_{1O}$	269.6	264.4	211.8	197.5
$t_{1\sigma}$	-20.7	25.4	-89.0	-106.4
$t_{1\perp}^a$	-25.6/-21.4	-11.9	-15.9/-10.5	-13.0
$t_{1\parallel}^b$	47.7/30.0	33.1	58.3/57.2	60.4
Distance	5.425 Å	5.427 Å	5.088 Å	5.096 Å
$t_{2O}$	-75.8	-77.0	-77.2	-78.7
$t_{2a}^b$	-3.5/-0.6	-1.4	-4.4/-5.3	-4.3
$t_{2b}$	-1.5	-1.4	0.1	1.4
$t_{2c}$	-36.5	-30.4	-24.9	-24.1
$t_{2d}^a$	12.5/10.2	9.3	18.4/17.9	18.7
$t_{2e}^a$	-21.4/-18.6	-19.0	-7.4/-7.8	-7.6

<sup>a</sup>For the shorter distance, the first number corresponds to  $xy \rightarrow xz$  and  $xy \rightarrow yz$  transitions and the second to  $xz \rightarrow yz$  transitions.

<sup>b</sup>For the shorter distance, the first number corresponds to  $xy \rightarrow xy$  transitions and the second number to  $xz \rightarrow xz$  and  $yz \rightarrow yz$  transitions.

spurious Hund's rule self-coupling of an orbital with itself. In particular, for the  $\approx 90^\circ$  geometry, as in this case, the Hund's rule coupling on oxygen is not supposed to promote ferromagnetism,<sup>18,21</sup> but in LDA and GGA it gives additional energetical advantage to the ferromagnetic state of the order of  $3I_O m_O^2/4 \approx 3 \times 1.6\text{eV} \times 0.1^2/4 \approx 12\text{meV}$  per Fe, where

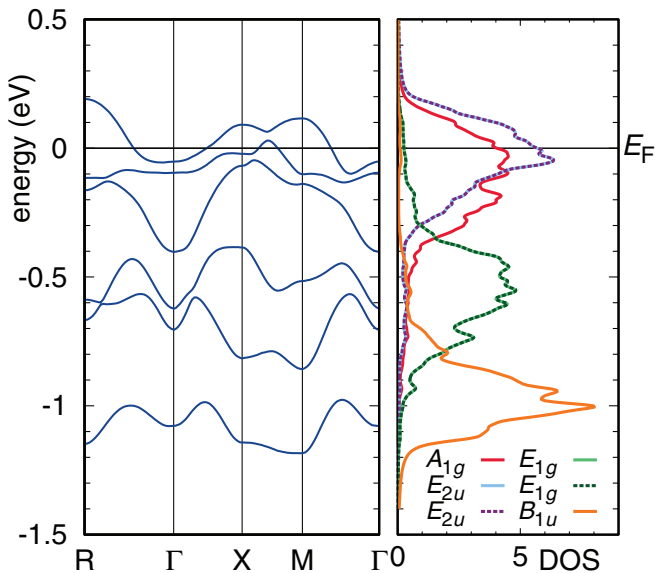


FIG. 4. (Color online) Nonrelativistic nonmagnetic band structure and density of states of  $\text{Li}_2\text{RhO}_3$ , projected onto quasimolecular orbitals, as described in Ref. 21.

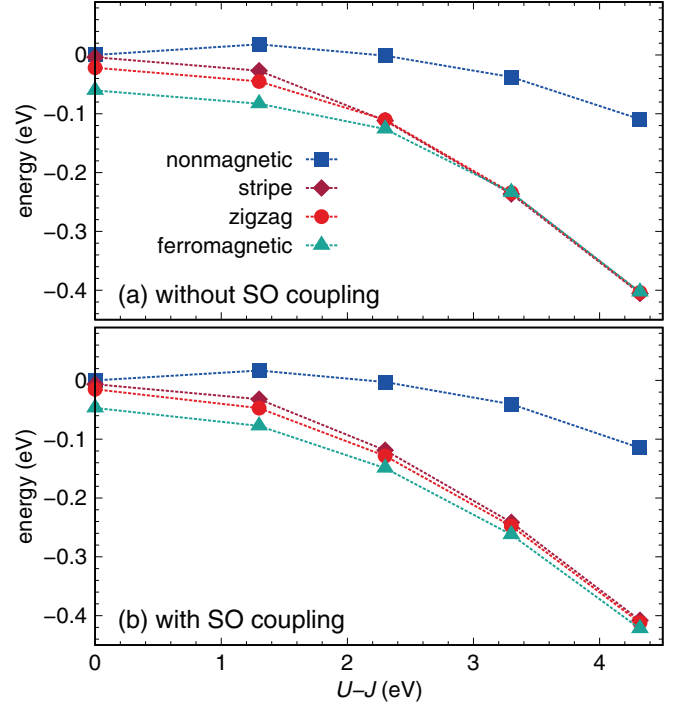


FIG. 5. (Color online) Energy of different magnetic configurations in eV/Rh relative to the nonmagnetic state, as a function of  $(U - J)$ . Energies at  $(U - J) \neq 0$  are offset by  $1.05(U - J)$ . (a) Without spin-orbit coupling. (b) With spin-orbit coupling.

$I_O = 1.6\text{eV}$  is the Stoner factor,<sup>32</sup>  $m_O = 0.1$  is the calculated magnetic moment of O, and there are three oxygens per Fe.

Neither the nonmagnetic state (Fig. 4) nor any of the magnetic states considered (FM, stripy, and zigzag) are insulating. Including SOC has little effect on either energetics or proximity to an insulator (Figs. 5–7).

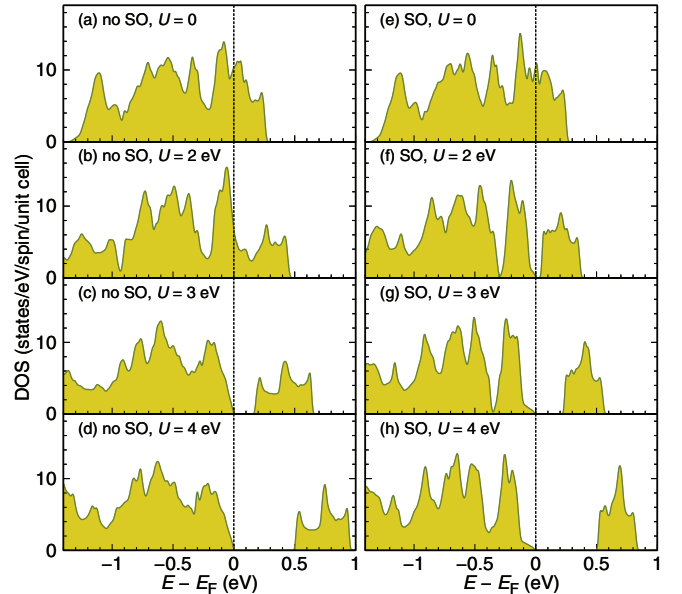


FIG. 6. (Color online) Evolution of the density of states with the Hubbard  $U$  in the zigzag phase without spin-orbit coupling (left panels) and with spin-orbit coupling (right panels). We use  $J_H = 0.7\text{eV}$  throughout.



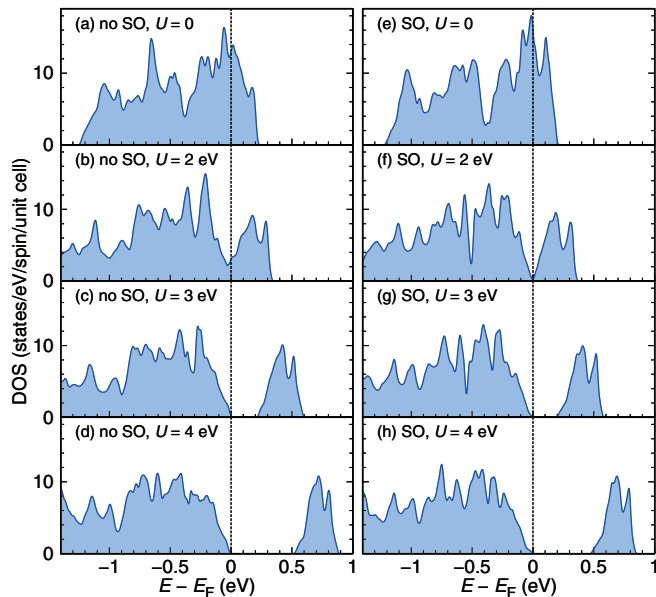


FIG. 7. (Color online) Evolution of the density of states with the Hubbard  $U$  in the stripy phase, without spin-orbit coupling (left panels) and with spin-orbit coupling (right panels). We use  $J_H = 0.7$  eV throughout.

On the other hand, experimentally this material appears to be insulating. It is natural to attribute this fact to the effect of Hubbard  $U$ , which in  $4d$  metals is about 3–4 eV, twice as large as for  $5d$  systems. Even though LDA + (onsite) $U$  is a rather naive way to tackle correlations in a QMO system, we have tried, *faut de mieux*, to apply a standard LDA +  $U$  correction to our calculations.<sup>33</sup> As expected, for  $U \gtrsim 3$  eV we obtain an insulator for both AFM configurations. In Figs. 6 and 7 we show the evolution of the density of states (DOS) with the Hubbard  $U$  for the zigzag and stripy configurations, respectively. Besides, adding  $U$  produces somewhat less obvious effects. First, it destabilizes the FM structure, making all three magnetic structures degenerate within the computational accuracy (in calculations with SOC the FM state is a few meV lower in energy, but, as mentioned, DFT always slightly overestimates this tendency because it includes Hund’s rule self-interaction on O). Second, the Hubbard  $U$  enhances the SOC, increasing the calculated orbital moments. The spin moment also positively correlates with  $U$ , but the dependence is much weaker. For instance, for the FM state the moment inside the Rh muffin-tin sphere increases from 0.58 to  $0.66\mu_B$  as  $U$  increases from 0 to 5 eV.

An important point to make is that, as one can expect from the small value of the SOC, it is not essential for obtaining an insulating state; an antiferromagnetic order, however, is, just as in such prototype Mott insulators as FeO and CoO. In fact, sometimes in LDA +  $U$  calculations including SOC is necessary for reproducing the insulating behavior, even though a material is obviously not relativistic. This is an artifact resulting from the inability of LDA +  $U$  to describe Mott insulators in the paramagnetic case. One of the pathologies that LDA +  $U$  shares with LDA is the absence of local magnetic fluctuations.<sup>34</sup> In both methods, instead of a

paramagnetic state, i.e., a state with disordered local moments, a non-magnetic state, with no moments at all, is considered. As a result, in such prototype strongly correlated materials as, for instance,  $3d$  oxides, a metallic state is protected by symmetry, unless some magnetic ordering is included (in some cases even the ferromagnetic order suffices; in others an antiferromagnetic ordering is needed), and LDA +  $U$  fails to reproduce the paramagnetic insulating phase.  $\text{Li}_2\text{RhO}_3$  is a similar case. In the nonmagnetic calculations there are band crossings protected by symmetry; that is to say, the best one can possibly achieve within LDA +  $U$ , even with an arbitrarily large  $U$ , is a zero-gap semiconductor. SOC, even infinitesimally small, removes this protection (the protected bands can now hybridize), and now a sufficiently large  $U$  can open a full gap. Obviously, this feature does not tell us anything about the real role of the SOC but only highlights shortcomings of the LDA +  $U$  method.<sup>35</sup> In fact, while the physics of  $\text{Na}_2\text{IrO}_3$  and  $\text{Li}_2\text{RhO}_3$  compounds is similar, the role of interactions is reversed. In the former, strong SOC renders the material nearly insulating already in the paramagnetic phase, and the relatively weak correlations only help the existing tendency. In the latter, for  $U = 0$  there exists already a sizable separation between the upper two bands but they are too wide and still overlap, forming a negative gap (see Fig. 4). Indeed, strong correlations are essential to open an actual gap, and the way to take correlations into account in LDA +  $U$  is to include magnetism from the very beginning. This scenario with the preexistence of a band separation is in contrast to the case of Mott insulators and corresponds to a correlated band insulator.

It is worth noting that the “213” honeycomb structure is peculiar in the sense that in the nearest-neighbor approximation the highest band is always a doublet, independent of the relative strength of the SOC. In the strong SOC limit this doublet is the relativistic  $j_{\text{eff}} = 1/2$ . In the opposite limit, this doublet is an  $A_{1g}$  molecular orbital, and the band structure can be characterized as an incipient band insulator. Mott-Hubbard correlations obviously enhance the tendency to insulating behavior but generally speaking are not always necessary. In real materials beyond this approximation the order of states may change, in which case SOC becomes absolutely essential (cf.  $\text{Na}_2\text{IrO}_3$ ), or bandwidth may become too large for such a simplistic treatment, but the fact that the most basic model has this unique feature is very important for understanding the physics of these honeycomb compounds. For a more detailed discussion we refer the reader to Ref. 21.

The observation that three different magnetic configurations, FM, zigzag, and stripy, with ordered moments on Rh ( $\sim 0.5$ – $0.7\mu_B$ ) independent of the magnetic pattern, are very close in energy indicates considerable frustration. Structural disorder is then expected to push the system toward a spin-glass regime.

These results show an important similarity between the  $5d$  compound  $\text{Na}_2\text{IrO}_3$  and the isostructural and isoelectronic  $4d$  compound  $\text{Li}_2\text{RhO}_3$ , despite a much larger Hubbard  $U$  and much smaller spin-orbit  $\lambda$  in the latter. This similarity suggests that properties of these materials are largely controlled by the nonrelativistic one-electron physics, namely, the formation of quasimolecular orbitals, while the role of

Coulomb correlations and SOC lies primarily in enhancing already existing tendencies (in particular, toward insulating behavior). As a word of caution, we want to emphasize that while our results point toward these systems being band (Slater) insulators rather than Mott insulators this does not indicate that they are weakly correlated or that they are localized rather than itinerant. On the other hand, our results suggest that local antiferromagnetism is an important ingredient in the formation of an insulating state and that Coulomb correlations are instrumental in enhancing the insulating gap.

## ACKNOWLEDGMENTS

We thank Yogesh Singh and Radu Coldea for collaboration and valuable discussions. R.V. and H.O.J. acknowledge support by the Deutsche Forschungsgemeinschaft through Grants No. SFB/TR 49 and No. FOR 1346. Work in Göttingen is supported by the Helmholtz Association through Project No. VI-521. S.M. acknowledges support from the Erasmus Mundus Eurindia Project. I.I.M. acknowledges funding from the Office of Naval Research (ONR) through the Naval Research Laboratory's Basic Research Program, and from the Alexander von Humboldt Foundation.

\*Present address: Oak Ridge National Laboratory, P.O. Box 2008, Oak Ridge, TN 37831-6114.

<sup>1</sup>S. J. Moon, H. Jin, K. W. Kim, W. S. Choi, Y. S. Lee, J. Yu, G. Cao, A. Sumi, H. Funakubo, C. Bernhard, and T. W. Noh, *Phys. Rev. Lett.* **101**, 226402 (2008).

<sup>2</sup>Y. Okamoto, M. Nohara, H. Aruga-Katori, and H. Takagi, *Phys. Rev. Lett.* **99**, 137207 (2007).

<sup>3</sup>B. J. Kim, H. Ohsumi, T. Komesu, S. Sakai, T. Morita, H. Takagi, and T. Arima, *Science* **323**, 1329 (2009).

<sup>4</sup>D. Pesin and L. Balents, *Nature Phys.* **6**, 376 (2010).

<sup>5</sup>Y. Singh and P. Gegenwart, *Phys. Rev. B* **82**, 064412 (2010).

<sup>6</sup>R. Comin, G. Levy, B. Ludbrook, Z.-H. Zhu, C. N. Veenstra, J. A. Rosen, Y. Singh, P. Gegenwart, D. Stricker, J. N. Hancock, D. van der Marel, I. S. Elfimov, and A. Damascelli, *Phys. Rev. Lett.* **109**, 266406 (2012).

<sup>7</sup>J. Chaloupka, G. Jackeli, and G. Khaliullin, *Phys. Rev. Lett.* **105**, 027204 (2010).

<sup>8</sup>I. I. Mazin, H. O. Jeschke, K. Foyevtsova, R. Valentí, and D. I. Khomskii, *Phys. Rev. Lett.* **109**, 197201 (2012).

<sup>9</sup>F. Gebhard, *The Mott Metal-Insulator Transition*, Springer Tracts in Modern Physics, Vol. 137 (Springer, New York, 1997).

<sup>10</sup>A. Georges, G. Kotliar, W. Krauth, and M. J. Rozenberg, *Rev. Mod. Phys.* **68**, 13 (1996).

<sup>11</sup>M. Imada, A. Fujimori, and Y. Tokura, *Rev. Mod. Phys.* **70**, 1039 (1998).

<sup>12</sup>M. R. Norman and J. P. Perdew, *Phys. Rev. B* **28**, 2135 (1983).

<sup>13</sup>E. G. Maksimov, I. I. Mazin, S. Y. Savrasov, and Y. A. Uspenski, *J. Phys.: Condens. Matter* **1**, 2493 (1989).

<sup>14</sup>K. Ohta, R. E. Cohen, K. Hirose, K. Haule, K. Shimizu, and Y. Ohishi, *Phys. Rev. Lett.* **108**, 026403 (2012).

<sup>15</sup>I. I. Mazin and V. I. Anisimov, *Phys. Rev. B* **55**, 12822 (1997).

<sup>16</sup>J. E. Pask, D. J. Singh, I. I. Mazin, C. S. Hellberg, and J. Kortus, *Phys. Rev. B* **64**, 024403 (2001).

<sup>17</sup>S. K. Choi, R. Coldea, A. N. Kolmogorov, T. Lancaster, I. I. Mazin, S. J. Blundell, P. G. Radaelli, Y. Singh, P. Gegenwart, K. R. Choi, S.-W. Cheong, P. J. Baker, C. Stock, and J. Taylor, *Phys. Rev. Lett.* **108**, 127204 (2012).

<sup>18</sup>J. Chaloupka, G. Jackeli, and G. Khaliullin, *Phys. Rev. Lett.* **110**, 097204 (2013).

<sup>19</sup>J. P. Clancy, N. Chen, C. Y. Kim, W. F. Chen, K. W. Plumb, B. C. Jeon, T. W. Noh, and Y.-J. Kim, *Phys. Rev. B* **86**, 195131 (2012).

<sup>20</sup>D. Haskel, G. Fabbris, M. Zhernenkov, P. P. Kong, C. Q. Jin, G. Cao, and M. van Veenendaal, *Phys. Rev. Lett.* **109**, 027204 (2012).

<sup>21</sup>K. Foyevtsova, H. O. Jeschke, I. I. Mazin, D. I. Khomskii, and R. Valentí, *Phys. Rev. B* **88**, 035107 (2013).

<sup>22</sup>Note that there is also an ongoing discussion about the nature of the insulating state in Sr<sub>2</sub>IrO<sub>4</sub>. See R. Arita, J. Kunes, A. V. Kozhevnikov, A. G. Eguluz, and M. Imada, *Phys. Rev. Lett.* **108**, 086403 (2012); Qing Li *et al.*, [arXiv:1303.7265](https://arxiv.org/abs/1303.7265).

<sup>23</sup>C. Martins, M. Aichhorn, L. Vaugier, and S. Biermann, *Phys. Rev. Lett.* **107**, 266404 (2011).

<sup>24</sup>V. Todorova and M. Jansen, *Z. Anorg. Allg. Chem.* **637**, 37 (2011).

<sup>25</sup>Y. Singh, S. Manni, J. Reuther, T. Berlijn, R. Thomale, W. Ku, S. Trebst, and P. Gegenwart, *Phys. Rev. Lett.* **108**, 127203 (2012).

<sup>26</sup>Y. Luo, C. Cao, B. Si, Y. Li, J. Bao, H. Guo, X. Yang, C. Shen, C. Feng, J. Dai, G. Cao, and Z.-A. Xu, *Phys. Rev. B* **87**, 161121 (2013).

<sup>27</sup>For initial optimization we used the VASP method<sup>36</sup> with the Perdew-Burke-Ernzerhof generalized gradient functional,<sup>37</sup> with the final adjustment using the all-electron WIEN2K code,<sup>28</sup> with default settings. The latter code was also used for the total-energy and DOS calculations.

<sup>28</sup>P. Blaha, K. Schwarz, G. K. H. Madsen, D. Kvasnicka, and J. Luitz, *WIEN 2K: An Augmented PlaneWave + Local Orbitals Program for Calculating Crystal Properties* (Karlheinz Schwarz, Techn. Universität Wien, Austria, 2001).

<sup>29</sup>M. Aichhorn, L. Pourovskii, V. Vildosola, M. Ferrero, O. Parcollet, T. Miyake, A. Georges, and S. Biermann, *Phys. Rev. B* **80**, 085101 (2009).

<sup>30</sup>J. Ferber, K. Foyevtsova, H. O. Jeschke, and R. Valentí, [arXiv:1209.4466](https://arxiv.org/abs/1209.4466).

<sup>31</sup>We double checked the agreement of total energies between linearized augmented plane wave and full potential local orbital.<sup>38</sup>

<sup>32</sup>I. I. Mazin and D. J. Singh, *Phys. Rev. B* **56**, 2556 (1997).

<sup>33</sup>We used LDA + *U* with the so-called fully localized limit double counting scheme and with the Hund's rule parameter  $J = 0.7$  eV.

<sup>34</sup>See, for example, L. Ortenzi, I. I. Mazin, P. Blaha, and L. Boeri, *Phys. Rev. B* **86**, 064437 (2012).

<sup>35</sup>Other recent work (Ref. 26 and C. Cao, Y. Luo, Z. Xu, and J. Dai, [arXiv:1303.4675](https://arxiv.org/abs/1303.4675)) reported first-principles calculation for the same compound, based on the VASP code. While their total-energy results agree with our WIEN2K results reasonably well, their nonrelativistic bands are more metallic in the LDA + *U* calculation, counterintuitively, and in contradiction to our results. Since these authors do not give many details of their calculations we could not trace the origin of this difference, but it is probably due to different cell dimensions used in that work.

<sup>36</sup>G. Kresse and J. Hafner, *Phys. Rev. B* **47**, 558 (1993); G. Kresse and J. Furthmüller, *Comput. Mater. Sci.* **6**, 15 (1996).

<sup>37</sup>J. P. Perdew, K. Burke, and M. Ernzerhof, *Phys. Rev. Lett.* **77**, 3865 (1996).

<sup>38</sup>K. Koepnick and H. Eschrig, *Phys. Rev. B* **59**, 1743 (1999).